Vapor−Liquid Equilibrium of CO_2 in Aqueous Solutions of 2-Amino-2-methyl-1-propanol†

Madhusree Kundu, Bishnu P. Mandal, and Syamalendu S. Bandyopadhyay*

Separation Science Laboratory, Cryogenic Engineering Centre, Indian Institute of Technology, Kharagpur 721302, India

The solubility of CO_2 in aqueous solutions, 18 mass %, 25 mass %, and 30 mass % (2.0 M, 2.8 M, and 3.4 M), of 2-amino-2-methyl-1-propanol (AMP) has been measured over a temperature range of (303 to 323) K and a partial pressure range of (1 to 100) kPa. In this work, the modified Clegg−Pitzer equation is used to correlate and predict the vapor−liquid equilibria of the (CO_2 + AMP + H_2O) system. The model predicted results are in good agreement with the experimental vapor−liquid equilibrium (VLE) measurements in this work. A nontraditional optimization algorithm, simulated annealing (SA), has been used for the parameter estimation. It is observed that adopting the SA technique for the estimation of interaction parameters results in better VLE prediction accuracy than using the traditional deterministic techniques, such as Levenberg−Marquardt.

Introduction

Removal of acid gas impurities such as CO_2 and H_2S from gas mixtures is very important in natural gas processing, hydrogen purification, and treating refinery off-gases and synthesis gas for manufacturing ammonia. Regenerative chemical absorption of the acid gases H_2S and CO_2 into solutions of alkanolamines, for example, monoethanolamine (MEA), diethanolamine (DEA), di-2-propanolamine (DIPA), and *N*-methyldiethanolamine (MDEA), is widely used for gas-treating processes. Recently a new class of amines, sterically hindered amines, has been introduced as a commercially attractive new absorbent.[1] Sharma[2] observed that the steric effect influences the stability of the carbamates formed due to the amine−CO_2 reaction and proposed the use of highly branched amines such as 2-amino-2-methyl-1-propanol (AMP) for higher cyclic absorption capacity for CO_2. AMP is considered today as one of the most important sterically hindered amines for natural gas treatment processes. As in MDEA, the CO_2 loading in AMP approaches a value of 1.0 mol of CO_2 per mole of amine, while the reaction rate constant for (CO_2 + AMP) is much higher than that for (CO_2 + MDEA).[3] Since the sterically hindered amine, AMP, does not form a stable carbamate,[3] bicarbonate and carbonate ions may be present in the solution in larger amounts than carbamate ions. Hence, the cost of regeneration energy when aqueous solutions of AMP are used to absorb CO_2 may be lower than when aqueous MDEA solutions are used.

Design of gas-treating processes by the traditional equilibrium stage approach requires a knowledge of vapor−liquid equilibrium (VLE) behavior of the aqueous acid gas + alkanolamine systems. In addition, equilibrium solubility of the acid gases in aqueous alkanolamine solutions determines the minimum recirculation rate of the solution that would treat a sour gas stream, and it determines the maximum concentration of acid gases which can be left in the regenerated solution in order to meet the product gas specifications. In rate-based models, physical and chemical equilibria play an important role by defining the boundary conditions for the partial differential equations that describe mass transfer coupled with chemical reactions. Representation of the experimental data with a thermodynamically rigorous model is required, so that one can systematically correlate and predict the vapor−liquid equilibria of these systems. A few results of CO_2 solubility in aqueous AMP solutions have been reported earlier (Roberts,[4] Teng and Mather,[5] Silkenbäumer et al.[6]). The recent literature on modeling the VLE of CO_2 and H_2S in single and mixed amine solvents includes the work of Kent and Eisenberg,[7] Li and Shen,[8] Deshmukh and Mather,[9] Austgen and Rochelle,[10] and Li and Mather.[11]

In this work, new experimental results of CO_2 solubility in (2.0, 2.8, and 3.4) M aqueous AMP solutions are reported in the temperature range of (303 to 323) K and at CO_2 partial pressures of (1 to 100) kPa. The Clegg−Pitzer equations are used to correlate and predict the vapor−liquid equilibria of the (AMP + CO_2 + H_2O) system. A nontraditional optimization algorithm like simulated annealing[12] was used for parameter estimation in the numerical part of the model solution for predicting the VLE of the acid gas + alkanolamine + water system.

Experimental Section

Chemicals. AMP was supplied by E. Merck, Germany, and had a purity of 98 mol %. Amine concentration was determined by titration with standard HCl using methyl orange indicator. Double-distilled water degassed by boiling was used to prepare aqueous amine solutions. A CO_2 cylinder was obtained from Hydrogas, India, and had 99.995 mol % certified purity. A N_2 cylinder was procured from BOC India and had a purity better than 99 mol %.

Apparatus. For VLE measurements, a stirred glass equilibrium cell was used. The experimental setup is shown in Figure 1. A magnetic stirrer was used for the liquid

† This contribution will be part of a special print edition containing papers presented at the 9th Asian Pacific Confederation of Chemical Engineering Congress, Christchurch, New Zealand, September 29 to October 3, 2002.

* Corresponding author. E-mail: ssbandyo@hijli.iitkgp.ernet.in. Fax: +91-3222-282258/255303.

10.1021/je0201626 CCC: $25.00
Published on Web 05/31/2003

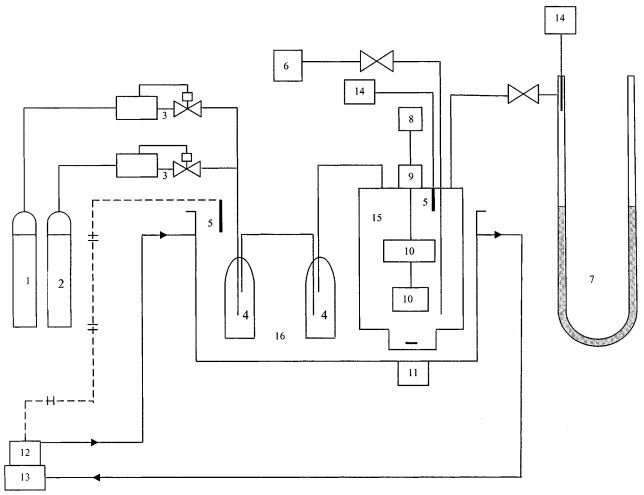

Figure 1. Schematic diagram of the VLE measurement setup: 1, CO_2 cylinder; 2, N_2 cylinder; 3, mass flow controller; 4, saturator; 5, Pt sensor; 6, gas chromatograph; 7, eudiometer tube; 8, dc drive; 9, mercury seal; 10, gas-phase stirrer; 11, magnetic stirrer; 12, temperature controller; 13, circulator; 14, temperature recorder; 15, stirred equilibrium cell; 16, thermostated water bath.

phase, and two four-bladed impellers mounted on a shaft, passing through a mercury seal and driven by a dc motor, were used for the gas phase. The temperature of the equilibrium cell was controlled within ±0.2 K of the desired level with a circulator temperature controller operated on external control mode (FP 55, Julabo, Germany). Precalibrated platinum sensors (Pt-100, Julabo) with indicator (Julabo TD300) were used for measurement of temperatures in the equilibrium cell, in the thermostated bath, and in the eudiometer tube. The uncertainty in the measurement of temperature was ±0.1 K. All VLE measurements were done at atmospheric pressure. A precise manometric device was employed to maintain atmospheric pressure in the cell throughout the equilibrium period. The total pressure was measured for each run within an accuracy of ±0.2 kPa. Precision mass flow controllers (Sierra Instruments, Monterey, CA) were used to control the flow rates of CO_2 and N_2.

Procedures. For each run, the equilibrium cell was allowed to reach thermal equilibrium at the desired temperature for the VLE measurement. The cell was then purged with the desired mixture of CO_2 and N_2. The N_2 and CO_2 gas streams at the outlet of the respective mass flow controllers were mixed and passed through water vapor saturators, maintained at the measurement temperature, before being introduced into the cell. Complete purging of the cell with dilute CO_2 of desired partial pressure was ensured by gas analysis at the inlet and outlet of the cell using a gas chromatograph (GC-16A, Shimadzu, Japan). The gas-phase stirrer was kept on at 70 rpm during purging to ensure uniform gas-phase concentration throughout the cell. After completion of purging, 10 mL of freshly prepared amine solution of desired concentration was quickly transferred in the cell and the cell was fully sealed. The liquid-phase and gas-phase stirrers were turned on to commence absorption. As absorption proceeded, CO_2 makeup from the pure CO_2 cylinder was carefully introduced into the cell through a fine control valve, precisely maintaining atmospheric pressure in the cell throughout the period of VLE measurements. The attainment of equilibrium was ensured when there was no absorption for at least 1 h while the temperature was maintained constant at the desired level. It took about (6 to 8) h to reach equilibrium for each run. After equilibrium was reached, gas-phase samples were analyzed by gas chromatography (GC-16A, Shimadzu), using Porapaq-Q and Porapaq-R columns connected in series, a TCD detector, and hydrogen carrier gas. The equilibrium CO_2 loading in the liquid phase was determined by acidulating known volumes of the loaded liquid samples with 6 M HCl and measuring the volume of the evolved gas. Determination of CO_2 in the liquid phase by evolution of CO_2 by acidulation has been done by several workers earlier (Hikita et al.,[13] Glasscock,[14] Glasscock et al.,[15] Saha et al.[3]). For the present work, the method was also standardized with several measurements using standard sodium carbonate test solutions and also with amine test solutions with a known CO_2 loading. The accuracy of the method has been found to be within ±2 %, and the reproducibility within 2 %. However, it was observed that accurate control and measurement of temperature in the desorption cell and eudiometer tube and precision in measuring the volume of evolved gas are very important to get accurate and reproducible results and minimize systematic error. The estimated experimental error in the measured solubility is about ±2 %. The experimental results of VLE measurement are presented in Tables 1−3.

Table 1. Solubility of CO_2 in 2 M AMP Solutions at 303 K

partial pressure/kPa	loading (α_{CO_2})	partial pressure/kPa	loading (α_{CO_2})
4.41	0.674	39.4	0.929
7.94	0.792	52.2	0.946
10.3	0.820	90.1	0.966
27.2	0.907		

Table 2. Solubility of CO_2 in 2.8 M AMP Solutions

T = 303 K		T = 313 K		T = 323 K	
partial pressure kPa	loading (α_{CO_2})	partial pressure kPa	loading (α_{CO_2})	partial pressure kPa	loading (α_{CO_2})
4.05	0.689	3.25	0.527	4.62	0.430
8.71	0.740	4.49	0.566	15.2	0.605
10.9	0.784	8.39	0.656	29.2	0.713
16.2	0.820	16.8	0.743	55.8	0.802
18.4	0.842	26.2	0.804	71.4	0.825
24.1	0.850	57.8	0.897	91.1	0.841
48.1	0.901	71.4	0.911		
58.0	0.911	91.5	0.924		
64.8	0.920				
76.2	0.932				
87.5	0.938				

Table 3. Solubility of CO_2 in 3.4 M AMP Solutions

T = 303 K		T = 313 K		T = 323 K	
partial pressure kPa	loading (α_{CO_2})	partial pressure kPa	loading (α_{CO_2})	partial pressure kPa	loading (α_{CO_2})
3.86	0.599	3.20	0.475	5.25	0.412
6.78	0.665	4.80	0.525	9.89	0.532
8.37	0.693	12.8	0.673	22.3	0.623
16.2	0.757	24.6	0.756	52.2	0.746
30.5	0.813	47.6	0.801	88.2	0.781
53.0	0.848	64.8	0.851		
94.0	0.889	93.0	0.876		

Modeling

Chemical Equilibria. In the aqueous phase for the AMP + CO_2 + H_2O system, the following chemical equilibria are involved.

$$CO_2 + H_2O \xleftrightarrow{K_{11}} H^+ + HCO_3^- \qquad (1)$$

$$\mathrm{AMP} + \mathrm{H_2O} \overset{K_{22}}{\longleftrightarrow} \mathrm{OH^-} + \mathrm{AMPH^+} \quad (2)$$

$$\mathrm{H_2O} \overset{K_{33}}{\longleftrightarrow} \mathrm{H^+} + \mathrm{OH^-} \quad (3)$$

Henry's law relates the acid gas partial pressure to the physically dissolved acid gas concentration in the solvent according to the following relation:

$$p_{\mathrm{CO_2}} = H_{\mathrm{CO_2}}[\mathrm{CO_2}] \quad (4)$$

The expression for thermodynamic equilibrium constants is as follows.

$$K_{11} = (m_{\mathrm{H^+}} m_{\mathrm{HCO_3^-}}/m_{\mathrm{CO_2}} m_{\mathrm{H_2O}})(\gamma^m_{\mathrm{H^+}}\, \gamma^m_{\mathrm{HCO_3^-}}/\gamma^m_{\mathrm{CO_2}}\, \gamma^m_{\mathrm{H_2O}}) \quad (5)$$

where m_i's are the molality of the species and γ_i^m's are the activity coefficients based on a molality scale.

$$K_{22} = (C_{\mathrm{OH^-}} C_{\mathrm{AMPH^+}}/C_{\mathrm{AMP}} C_{\mathrm{H_2O}})(\gamma^c_{\mathrm{OH^-}}\, \gamma^c_{\mathrm{AMPH^+}}/\gamma^c_{\mathrm{AMP}}\, \gamma^c_{\mathrm{H_2O}}) \quad (6)$$

$$K_{33} = (C_{\mathrm{H^+}} C_{\mathrm{OH^-}}/C_{\mathrm{H_2O}})(\gamma^c_{\mathrm{H^+}}\, \gamma^c_{\mathrm{OH^-}}/\gamma^c_{\mathrm{H_2O}}) \quad (7)$$

where C_i's are the molarity of the species and γ_i^c's are the activity coefficients based on a molarity scale.

The thermodynamic equilibrium constant K_{11} is based on a molality scale, and K_{22} and K_{33} are given on a molarity scale. All are considered to be functions of temperature. The Henry's constant (H) has the unit of pascals and is considered to be a function of temperature. The functional form of the temperature dependence and the temperature coefficients for both equilibrium constants and Henry's constant are taken from the literature as shown in Table 4.

From eqs 2 and 3, we can write

$$\mathrm{AMPH^+} + \mathrm{H_2O} \overset{K_2'}{\longleftrightarrow} \mathrm{AMP} + \mathrm{H^+} \quad (8)$$

$$K_2' = \frac{K_{33}}{K_{22}} \quad (9)$$

where K_2' is the thermodynamic equilibrium constant for eq 8 and is based on a molarity scale. To use those thermodynamic equilibrium constants in the present model, the equilibrium constants K_{11} and K_2' are converted to mole fraction based equilibrium constants in the following way.

$$K_1 = K_{11}(M_s/1000) \quad (10)$$

$$\ln K_1 = \ln K_{11} - \ln(1000/M_s) \quad (11)$$

$$K_2 = K_2'(M_s/1000\rho) \quad (12)$$

$$\ln K_2 = \ln K_2' - \ln(1000\rho/M_s) \quad (13)$$

where K_1 and K_2 are the mole fraction based equilibrium constants for eqs 1 and 8, respectively. M_s is the molecular mass of the pure solvent, and ρ is the density of the pure solvent. In general, to convert the logarithm of an equilibrium constant for the dissociation of an electrolyte in water from the molality scale to the mole fraction scale, it is necessary to subtract $\ln(1000/M_s)$ for each nonwater component on the right-hand side of a stoichiometric expression and to add $\ln(1000/M_s)$ for each nonwater component on the left-hand side of a stoichiometric expression, as shown in eq 11. In the case of conversion from the molarity scale to the mole fraction scale, the subtraction and addition factor is $\ln(1000\rho/M_s)$, as shown in eq 13.

There are only four main species, two neutral solvents, AMP and H_2O, and two ionic species, $AMPH^+$ and HCO_3^-, in the equilibrated liquid phase. To reduce the complexity, the presence of free molecular species of CO_2 and the ionic species OH^- and CO_3^{2-} in the equilibrated liquid phase were neglected, since concentrations of these species are very low compared to the other species present in the equilibrated liquid phase. Several previous workers (Li and Mather,[11,16] Haji-Sulaiman et al.,[17] Posey[18]) have observed that neglecting the concentrations of free molecular CO_2 and OH^- and CO_3^{2-} ions in the liquid phase in this system for a CO_2 loading below 1.0 does not result in significant error in the VLE predictions. It is thus assumed that all the dissolved CO_2 is converted into HCO_3^- ions. The vapor phase has been assumed to be ideal, as the present results are limited to low to moderate pressures. From eqs 1, 4, and 8, we get the expression for the equilibrium partial pressure of CO_2 over an aqueous AMP solution.

$$P_{\mathrm{CO_2}}/\mathrm{kPa} = (H_{\mathrm{CO_2}} K_2 x_{\mathrm{AMPH^+}} \gamma_{\mathrm{AMPH^+}} x_{\mathrm{HCO_3^-}} \gamma_{\mathrm{HCO_3^-}})/(K_1 x_{\mathrm{H_2O}} x_{\mathrm{AMP}} \gamma_{\mathrm{H_2O}} \gamma_{\mathrm{AMP}}) \quad (14)$$

x_n's are the liquid-phase mole fractions, based on true molecular or ionic species. Activity coefficients γ_I's (based on the mole fraction scale) for different species present in the liquid phase are calculated from the modified Clegg−Pitzer equation according to the method proposed by Li and Mather.[11]

Thermodynamic Expression. In the modified Pitzer equation, all the species in a system are considered as interacting particles. The excess Gibbs energy arises from inequalities in interparticle forces. The excess Gibbs energy is assumed to consist of short-range forces and long-range Debye−Huckel forces.

$$g^{\mathrm{E}} = g^{\mathrm{S}} + g^{\mathrm{DH}} \quad (15)$$

For a short-range term, only two- and three-suffix Margules expansions are used,

$$g^{\mathrm{S}}/RT = x_I \sum x_n \sum_c \sum_a F_c F_a W_{nca} + \sum_n \sum_{n'} x_n x_{n'} (A_{n'n} A_{nn'} x_{n'}) \quad (16)$$

where c, a, n, and n' represent cation, anion, and neutral species and g^{S} is the short-range contribution to the excess Gibbs energy. The total mole fraction of ions (x_I) is given by

$$x_I = \text{total mole fraction of ions} = 1 - \sum_n x_n \quad (17)$$

The cation and anion fraction F_c and F_a are defined for fully symmetrical systems by

$$F_c = 2\frac{x_c}{x_I} \quad (18)$$

$$F_a = 2\frac{x_a}{x_I} \quad (19)$$

$A_{n'n}$ and $A_{nn'}$ are solvent−solvent interaction parameters. W_{nca} are the ion−solvent interaction parameters. For the long-range contribution to the excess Gibbs energy, the

Table 4. Temperature Dependence of the Equilibrium Constants for Reactions 1−3 and Henry's Constant for CO_2

$$\ln K_{11} = A/T + B \ln T + CT + D$$

$$\ln K_{22} = A/T + B \ln T + CT + D$$

$$\ln K_{33} = A + B/T + C/T^2 + D/T^3 + E/T^4$$

$$\ln H = A + B/T + C \ln T + DT$$

	A	*B*	*C*	*D*	*E*	ref
reaction 1	−7742.6	−14.506	-2.8104×10^{-2}	102.28		6
reaction 2	−7261.78	−22.4773	0	142.58612		6
reaction 3	39.5554	-9.879×10^4	0.568827×10^8	-0.14645×10^{11}	0.136145×10^{13}	8
Henry's constant	170.7126	−8477.711	−21.95743	0.005781		11

following expression is used:

$$g^{DH}/RT = (-4A_x I_x/\Omega \ln(1 + \Omega I_x^{1/2})) + \sum_c \sum_a x_c x_a B_{ca} g(\alpha_1 I_x^{1/2}) \quad (20)$$

where B_{ca} is the ion−ion interaction parameter and (I_x) is the mole fraction ionic strength,

$$I_x = 0.5 \sum z_i^2 x_i \quad (21)$$

The function $g(x)$ is expressed by

$$g(x) = 2[1 - (1 + x) \exp(-x)]/x^2 \quad (22)$$

where

$$x = (\alpha_1 I_x^{1/2}) = 2I^{1/2} \quad (23)$$

and I is the ionic strength in molar concentration, and the Debye−Huckel parameter on mole fraction basis is given by

$$A_x = A_\phi (\sum_n C_n)^{1/2} \quad (24)$$

where C_n is the molar concentration of the solvent n, A_ϕ is the original Debye−Huckel parameter and a function of temperature, density, and relative permittivity of the mixed solvent. The parameter Ω is related to the hard-core collision diameter and given by the relation

$$\Omega = 2150\{(18.02 \times \rho_m \sum_n C_n)/(1000 \times \epsilon_m T)\}^{1/2} \quad (25)$$

where ρ_m is the density of the mixed solvent.

The relative permittivity (ϵ_m) of the mixed solvents is

$$(\epsilon_m) = \sum_n \phi_n \epsilon_n \quad (26)$$

where ϕ_n is the volume fraction of solvent n.

$$\phi_n = (C_n V_n / \sum_n C_n V_n) \quad (27)$$

The temperature dependence of density of the pure solvents is listed in Table 5. As AMP is methyl-substituted MEA, the relative permittivity of AMP is assumed here as that of MEA. The temperature dependence of the relative permittivity for pure solvents is presented in Table 6. Differentiation of eqs 16 and 20 yields the expressions for the short-range and long-range force contribution to the activity coefficients of ions and neutral species.

Table 5. Temperature Dependence of the Density of the Pure Solvents

solvent	MW	expression	*t* range °C
H_2O[a]	18.02	$\rho = 0.999382 + 0.00007208t - 7.28491 \times 10^{-6}t^2 + 2.65177 \times 10^{-8}t^3$	20−80
AMP[b]	89.14	$\rho = 1.1851 - 8.53143 \times 10^{-4}t$	20−80

[a] Li and Mather (ref 11). [b] Derived empirical relation from experimental data.

Table 6. Temperature Dependence of the Relative Permittivity of the Pure Solvents

solvent	expression	*t* range °C
H_2O[a]	$\epsilon = 78.54[1 - 4.579 \times 10^{-3}(t - 25) + 1.19 \times 10^{-5}(t - 25)^2 - 2.8 \times 10^{-8}(t - 25)^3$	0−100
MEA[a]	$\epsilon = 35.76 + 14836(1/(t + 273) - 1/273.15)$	−70−60

[a] Li and Mather (ref 11).

Table 7. Experimental Solubility Data Used in the Regression Analysis to Estimate the Interaction Parameters and Determine the Correlation Deviations for the AMP + CO_2 + H_2O Ternary System

reference	[AMP] M	*T* K	data points	AAD%[a]
Teng and Mather (ref 5)	2.0	313	15	16.0
Li and Chang (ref 22)	3.4	333, 353, 373	36	9.34
this study	2.8	303	14	13.0

[a] AAD% = $\sum_n [(p_{cal} - p_{exp}) \times 100/p_{exp}]/n$.

Estimation of the Interaction Parameter

In this work, the experimental solubility data comprising acid gas loadings in the range of (0.03 to 1.0) mol/mol and the partial pressures of acid gas in the range of (0.300 to 1000) kPa have been used to estimate the interaction parameters by regression analysis. The optimization of the objective function was done by both the simulated annealing (SA) technique and a traditional optimization technique, Levenberg−Marquardt (LM). The objective function for regression is

$$\psi = \sum |\{(P_{CO_2})_{cal} - (P_{CO_2})_{exp}\}/(P_{CO_2})_{exp}| \quad (28)$$

The VLE data used for regression analysis along with their average correlation deviation have been summarized in Table 7. In the SA technique, the five interaction parameters were estimated by the regression analysis over the temperature range of (303 to 373) K. Among the interaction

Table 8. Estimated Interaction Parameters for the AMP + CO_2 + H_2O System within a 95% Confidence Interval

B or W or A[a]	T = 333 K	T = 353 K	T = 373 K
W_{1MX}	2.000 ± 0.47	3.000 ± 0.10	5.000 ± 0.38
W_{2MX}	16.00 ± 2.00	17.49 ± 1.10	22.26 ± 4.90
B_{MX}	−15.74 ± 0.23	−14.80 ± 0.02	−6.108 ± 0.20
A_{12}	32.42 ± 5.02	35.69 ± 2.40	45.02 ± 7.05
A_{21}	−14.03 ± 2.21	−18.30 ± 2.40	−18.62 ± 5.10

[a] Subscripts: 1 = AMP, 2 = H_2O, M = $AMPH^+$, X = HCO_3^-.

Table 9. Fitted Values of the Interaction Parameters for the AMP + CO_2 + H_2O System

$$B \text{ (or } W \text{ or } A) = a + bT + cT^2$$

B or W or A[a]	a	b	c
W_{1MX}	163.654	−0.984 56	0.001 50
W_{2MX}	−20.2805	0.110 78	0
B_{MX}	−140.466	0.361 05	0
A_{12}	−43.0574	0.230 11	0
A_{21}	23.5064	−0.115 00	0

[a] Subscripts: 1 = AMP, 2 = H_2O, M = $AMPH^+$, X = HCO_3^-.

parameters, one is for ion−ion interactions, two are for ion−solvent interactions, and two are for solvent−solvent interactions. While the VLE prediction accuracies have been found to be very good, the statistical determination of accuracy of the estimated parameters was reasonably good. The 95% confidence intervals of the five interaction parameters are listed in Table 8. Later, the functional form of their temperature dependence was derived. The five interaction parameters were fitted to the linear/polynomial functionality of temperature with an average regression coefficient of 0.99 ± 0.01. The temperature coefficients of the parameters are listed in Table 9. For the LM technique, the regression analysis was done along with the temperature coefficients relating the interaction parameters. This difference in regression analysis between the SA and LM techniques was made only to reduce the execution time in the case of the SA technique. Since no reliable experimental data for the binary system (AMP + H_2O) are available, the solvent−solvent interaction parameters were also estimated with the solubility data for the ternary system (AMP + CO_2 + H_2O).

Method of Solution

The problem of parameter estimation in the model predicting VLE of an aqueous acid gas + alkanolamine system involves regression of experimental data wherein optimum values of the parameters are found. In this paper, the regression function has been considered to be an objective function that is to be minimized. SA is a computational stochastic technique for finding near global minimum solutions to optimization problems. The method mimics the thermodynamic process of cooling of molten metals for achieving the minimum free energy state. The main driving force behind SA is to occasionally allow for wrong-way movement (uphill moves for minimization) simultaneously providing convergence to the global optimum. The SA method works with a point in the variable search space of the vector according to the Boltzmann probability distribution, given by

$$P = \exp\left(\frac{-\Delta E}{k_B T}\right) \tag{29}$$

where k_B is the Boltzmann constant and T is the current annealing temperature.

The energy function becomes the objective function. The particle configurations are the variable values. Finding a low-energy configuration becomes seeking a near optimal solution for the function where temperature becomes a control parameter for the solution. This leads to the generation of a Markov Chain of points that are given by distribution eq 29 and are independent of the initial point. The acceptance criterion given by eq 29 is referred to as the Metropolis criterion for SA. This expression suggests that a system at a high temperature has almost uniform probability of being at a high-energy state, but at low temperature it has a small probability of being at a high-energy state. Therefore, by controlling the temperature T and assuming the search process follows the Boltzmann probability distribution, the convergence of the algorithm can be controlled. In the course of simulations, the temperature is systematically annealed using a schedule like Kirkpatrick's exponential schedule,[19]

$$T_{i+1} = \xi T_i \tag{30}$$

where ξ is the cooling factor and $0.9 \le \xi \le 1.0$. The move schedule for consideration of a given number of configurations at each temperature is done using a random schedule. The choice of such schedules varies along with the problem being considered. SA is a point-by-point method. The algorithm begins with an initial point and a high temperature T. A second point is created at random in the vicinity of the initial point, and the difference in the function values (ΔE) at these two points is calculated. If the second point has a smaller function value, the point is accepted; otherwise the point is accepted with a probability ($-\Delta E/T$). This completes one iteration of the SA procedure. To simulate the thermal equilibrium at every temperature, a number of points n are usually tested at a particular temperature, before reducing the temperature. The algorithm is terminated when a sufficiently small temperature is obtained or a small enough change in function values is found. The initial temperature T and the number of iterations performed at a particular temperature are two important parameters, which govern the successful working of the simulated annealing procedure. The algorithm flowchart is given in Figure 2.

Results and Discussion

The fitted interaction parameters and the correlation presented in Tables 8 and 9 for the AMP + CO_2 + H_2O ternary system on the basis of the experimental solubility data set, presented in Table 7, have been used here to predict some solubility data for a range of temperature and solvent composition. These data were not used for the regression. These predictions are summarized in Table 10 and Figures 3−7 and presented in the figures as model predicted curves. However, Figures 3, 4, and 7 also include correlated solubility curves to show the correlation deviation with the experimental solubility data, which were used for the regression. In Figures 3, 4, and 7, these results are shown by correlation curves. For modeling of the vapor−liquid equilibrium of CO_2 + alkanolamine + water systems, average deviations in the range of 15 to 30% have been reported by previous workers (Silkenbäumer et al.,[6] Li and Shen,[8] Deshmukh and Mather,[9] Austgen and Rochelle,[10] Li and Mather[11,16]), who used deterministic techniques for modeling. In this work, the SA technique was employed in order to achieve better VLE prediction accuracy. In a relative evaluation of the LM and SA techniques for

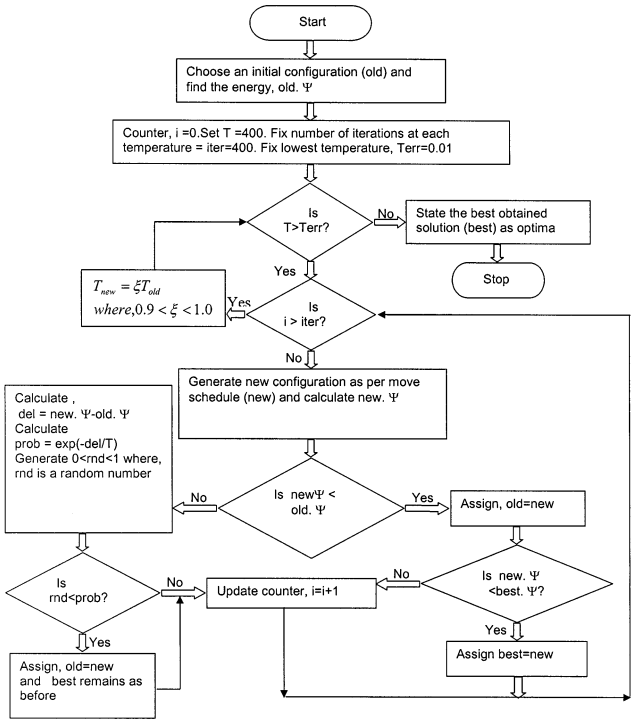

Figure 2. Flowchart for the simulated annealing (SA) algorithm.

Table 10. Average Deviation for Prediction of Solubility in the AMP + CO_2 + H_2O System by the SA Technique

reference	[AMP]/M	*T*/K	data points	AAD %[a]
Teng and Mather (ref 5)	2.0	343	9	22.3
Jane and Li (ref 21)	2.0	313	7	20.0
Roberts (ref 4)	2.0, 3.0	313	15	17.6
Seo and Hong (ref 23)	3.4	313, 333, 353	19	15.7
Silkenbäumer et al. (ref 6)	5.96, 5.64	313, 333	16	18.9
this study	2.0, 2.8, 3.4	303, 313, 323	56	14.3

[a] $AAD\% = \sum_n[(p_{cal} - p_{exp}) \times 100/p_{exp}]/n$.

Table 11. Average Deviation for Prediction of Solubility in the AMP + CO_2 + H_2O System by the LM Technique

reference	[AMP]/M	*T*/K	data points	AAD %[a]
Jane and Li (ref 21)	2.0	313	7	23.5
Roberts (ref 4)	2.0, 3.0	313	15	15.2
Seo and Hong (ref 23)	3.4	313, 333, 353	20	18.2
this study	2.0, 2.8, 3.4	303, 313, 323	56	18.0

[a] $AAD\% = \sum_n[(p_{cal} - p_{exp}) \times 100/p_{exp}]/n$.

parameter estimation, it was found by Kundu and Bandyopadhyay[20] that the SA technique resulted in better accuracy in prediction of VLE. The average absolute deviation percent of prediction of VLE in the AMP + CO_2 + H_2O system by the SA and LM techniques is summarized in Tables 10 and 11, respectively. However, the execution time and the number of function evaluation were understandably higher for a probabilistic algorithm like SA, in comparison to LM technique. The hardware platform used was an Intel Pentium-III processor, 701 MHz for all the runs, for both of the techniques.

Correlation and prediction results are shown in Figures 3−7. For 2 M AMP solutions, the experimental data of CO_2 solubility from Teng and Mather[5] and of this study have been compared with the model predicted results for the temperatures (303 and 343) K, as shown in Figure 3. Figure 3 also presents a correlated solubility curve at 313 K, based

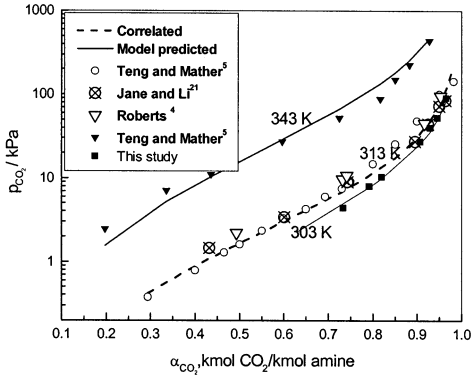

Figure 3. Equilibrium partial pressure of CO_2 over 2 M AMP solutions.

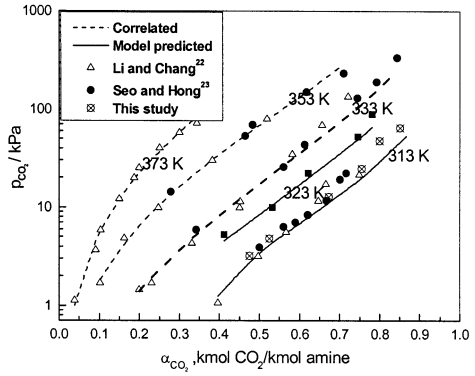

Figure 4. Equilibrium partial pressure of CO_2 over 3.4 M AMP solutions.

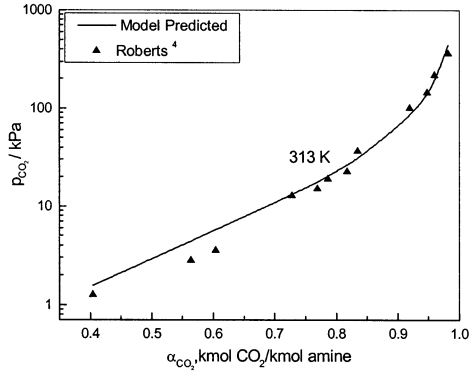

Figure 5. Equilibrium partial pressure of CO_2 over 3.0 M AMP solutions.

on the experimental solubility data of Teng and Mather,[5] Roberts,[4] and Jane and Li.[21] The related correlation deviation for this is presented in Table 7. As shown in Figure 4, there is a reasonable agreement between correlated as well as model predicted results and the experimental data for the solubility of CO_2 in 30 mass % (3.4 M) AMP solution over a temperature range of (313 to 373) K. The fitted interaction parameters have been used to predict the solubility of CO_2 in 3 M AMP at 313 K, in 5.96 M AMP at 333 K, and in 5.64 M AMP at 313 K. As shown in Figures 5 and 6, the model predicted equilibria are found to be in good agreement with the experimental results of Roberts[4] and Silkenbäumer et al.,[6] respectively. The experimental solubility data of CO_2 in 2.8 M AMP at (313 and 323) K have been compared with the predicted CO_2 solubility in Figure 7. This also presents the correlated solubility curve at 303 K along with the experimental data, which were

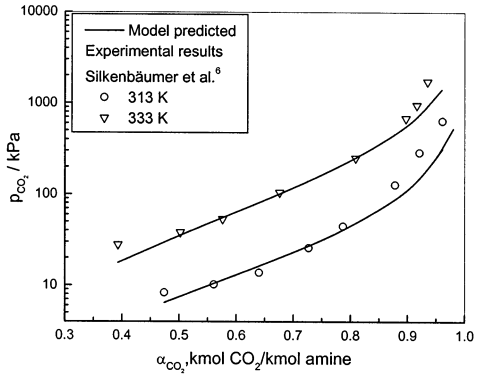

Figure 6. Equilibrium partial pressure of CO_2 over 5.96 and 5.64 M AMP solutions.

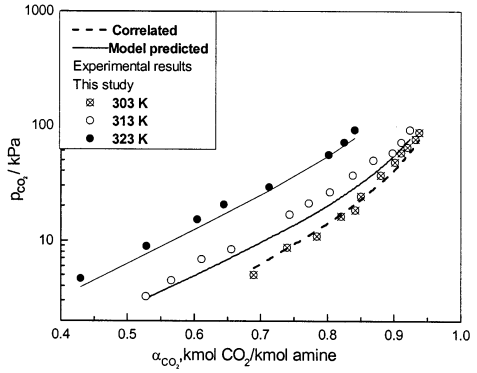

Figure 7. Equilibrium partial pressure of CO_2 over 2.8 M AMP solutions.

used for correlation. In all the cases, the agreement is excellent.

Conclusions

The equilibrium solubility of CO_2 in aqueous solutions of AMP was measured in the temperature range of (303 to 323) K for a CO_2 partial pressure range of (1 to 100) kPa. The equilibrium solubility of CO_2 in aqueous AMP solutions has been correlated with a simplified Clegg−Pitzer equation. The model predicted partial pressures of CO_2 over aqueous AMP solutions have been found to be in good agreement with the experimental results of this study and results available in the open literature. This provides additional support for the validity of the experimental technique. Simulated annealing has been successfully implemented for parameter estimation of the VLE model. Better accuracy of the predicted results in comparison to traditional deterministic techniques establishes the utility of nontraditional optimization algorithms such as simulated annealing in the estimation of parameters.

Nomenclature

H_{CO_2}	Henry's law constant, Pa
K_1, K_2	thermodynamic chemical equilibrium constant, expressed in activity and in mole fraction
K_2', K_{22}, K_{33}	thermodynamic chemical equilibrium constant, expressed in activity and in molarity
K_{11}	thermodynamic chemical equilibrium constant, expressed in activity and in molality
z_i	valency of an ion
g^E	excess Gibbs free energy
g^S	short-range force contribution to the excess Gibbs free energy
g^{DH}	long-range force contribution to the excess Gibbs free energy
p_{CO_2}	partial pressure of CO_2, Pa or kPa
T	absolute temperature, K
t	temperature, °C
C	molar concentration
ρ	density of pure solvent
M_s	molecular weight of pure solvent
F	ionic fraction
I	ionic strength on molality basis
I_x	ionic strength on mole fraction basis
R	gas constant
ϵ	relative permittivity
$A_{nn'}$	interaction parameter between neutral molecules
W	interaction parameter between neutral and ionic species
A_x	Debye−Huckel parameter on mole fraction basis
A_ϕ	Debye−Huckel parameter for osmotic coefficient

Greek Letters

(α_1)	Pitzer universal constant in eq 20
α_{CO_2}	liquid-phase loading of CO_2, kmol CO_2/kmol amine
γ	activity coefficient
ϕ	volume fraction
Ω	hard-core collision diameter
ψ	objective function for regression

Superscripts

S	short-range term
DH	long-range term

Subscripts

a, X	anion
c, M	cation
n,n'	neutral solvent species
cal	calculated value
exp	experimental value

Literature Cited

(1) Sartori, G.; Savage, D. W. Sterically Hindered Amines for CO_2 Removal from Gases. *Ind. Eng. Chem. Fundam.* **1983**, *22*, 239−249.
(2) Sharma, M. M. Kinetics of Gas Absorption. Absorption of CO_2 and COS in Alkaline and Amine Solutions. Ph.D. Thesis, University of Cambridge, Cambridge, U.K., 1964; *Trans. Faraday. Soc.* **1965**, *61*, 681−688.
(3) Saha, A. K.; Bandyopadhyay, S. S.; Biswas, A. K. Kinetics of Absorption of CO_2 in to Aqueous Solutions of 2-Amino-2-methyl-1-propanol. *Chem. Eng. Sci.* **1995**, *50*, 3587−3598.
(4) Roberts, B. E. Solubility of CO_2 and H_2S in Chemical and Mixed Solvents. M.Sc. Thesis, University of Alberta, Edmonton, Alberta, Canada, 1983.
(5) Teng, T. T.; Mather, A. E. Solubility of H_2S, CO_2 and Their Mixtures in an AMP Solution. *Can. J. Chem. Eng.* **1989**, *67*, 846−850.
(6) Silkenbäumer, D.; Rumpf, B.; Lichtenthaler, R. N. Solubility of Carbon Dioxide in Aqueous Solutions of 2-Amino-2-methyl-1-propanol and *N*-methyldiethanolamine and Their Mixtures in the Temperature Range from 313 to 353 K and Pressure up to 2.7 MPa. *Ind. Eng. Chem. Res.* **1998**, *37*, 3133−3141.
(7) Kent, R. L.; Eisenberg, B. Better Data for Amine Treating. *Hydrocarbon Process.* **1976**, *55* (2), 87−90.
(8) Li, M. H.; Shen, K. P. Calculation of Equilibrium Solubility of Carbon Dioxide in Aqueous Mixtures of Monoethanolamine with Methyldiethanolamine. *Fluid Phase Equilib.* **1993**, *85*, 129−140.
(9) Deshmukh, R. D.; Mather, A. E. A Mathematical Model for Equilibrium Solubility of Hydrogen Sulfide and Carbon Dioxide in Aqueous Alkanolamine Solutions. *Chem. Eng. Sci.* **1981**, *36*, 355−362.

(10) Austgen, D. M.; Rochelle, G. T. Model of Vapor−Liquid Equilibria for Aqueous Acid Gas−Alkanolamine Systems. 2. Representation of H_2S and CO_2 Solubility in Aqueous MDEA and CO_2 Solubility in Aqueous Mixture of MDEA with MEA or DEA. *Ind. Eng. Chem. Res.* **1991**, *30*, 543−555.

(11) Li, Y. G.; Mather, A. E. Correlation and Prediction of the Solubility of Carbon Dioxide in a Mixed Alkanolamine Solution. *Ind. Eng. Chem. Res.* **1994**, *33*, 2002−2005.

(12) Aarts, E.; Korst, J. *Simulated Annealing and Boltzmann Mechanics*: *A Stochastic Approach to Combinatorial Optimization and Neural Computing*; Wiley: Chichester, 1989.

(13) Hikita, H.; Asai, S.; Katsu, Y.; Ikuno, S. Absorption of Carbon Dioxide into Aqueous Monoethanolamine Solutions. *AIChE J.* **1979**, *25* (5), 793−800.

(14) Glasscock, D. A. Modelling and Experimental Study of Carbon Dioxide Absorption into Aqueous Alkanolamine. Ph.D. Thesis, University of Texas, Austin, TX, 1990.

(15) Glasscock, D. A.; Critchfield, J. E.; Rochelle, G. T. CO_2 Absorption/Desorption in Mixtures of Methyldiethanolamine with Monoethanolamine or Diethanolamine. *Chem. Eng. Sci.* **1991**, *46*, 2829−2845.

(16) Li, Y. G.; Mather, A. E. Correlation and Prediction of the Solubility of CO_2 and H_2S in Aqueous Solutions of Methyldiethanolamine. *Ind. Eng. Chem. Res.* **1997**, *36*, 2760−2765.

(17) Haji-Sulaiman, M. Z.; Aroua, M. K.; Pervez, M. I. Equilibrium concentration profiles of species in CO_2−Alkanolamine−Water Systems. *Gas. Sep. Purif.* **1996**, *10*, 13−18.

(18) Posey, M. L. Thermodynamic Model for Acid Gas Loaded Aqueous Alkanolamine Solutions. Ph.D. Thesis, University of Texas, Austin, TX, 1996.

(19) Kirpatrick, S.; Gelatt, C. D.; Vecchi, M. P. Optimization by Simulated Annealing. *Science* **1983**, *220*, 671−680.

(20) Kundu, M.; Bandyopadhyay, S. S. A Comparative Study of Deterministic and Probabilistic Algorithms for Predicting Vapor−Liquid Equilibria in CO_2−AMP−Water System. Presented at the Indian Chemical Engineering Congress (CHEMCON 2002), December, 2002, Hyderabad, India.

(21) Jane, I. S.; Li, M. H. Solubilities of Mixtures of Carbon Dioxide and Hydrogen Sulfide in Water + Diethanolamine + 2-Amino-2-methyl-1-propanol. *J. Chem. Eng. Data* **1997**, *42*, 98−105.

(22) Li, M. H.; Chang, B. C. Solubilities of Carbon Dioxide in Water + Monoethanolamine + 2-Amino-2-methyl-1-propanol. *J. Chem. Eng. Data* **1994**, *39*, 448−452.

(23) Seo, D. J.; Hong, W. H. Solubilities of Carbon Dioxide in Aqueous Mixtures of Diethanolamine and 2-Amino-2-methyl-1-propanol. *J. Chem. Eng. Data* **1996**, *41*, 258−260.

Received for review August 21, 2002. Accepted March 21, 2003. This work was supported by the Centre for High Technology (CHT), New Delhi, India.

JE0201626